NANO LETTERS

Letter

pubs.acs.org/NanoLett

# Vesicle Fusion Triggered by Optically Heated Gold Nanoparticles

Andreas Rørvig-Lund,[†] Azra Bahadori,[†,‡] Szabolcs Semsey,[†] Poul Martin Bendix,*[,†] and Lene B. Oddershede*[,†,‡]

[†]Niels Bohr Institute, University of Copenhagen, Blegdamsvej 17, 2100 Copenhagen, Denmark

[‡]Lundbeck Foundation Center of Excellence for Biomembranes in Nanomedicine, University of Copenhagen, Copenhagen, Denmark

Supporting Information

**ABSTRACT:** Membrane fusion can be accelerated by heating that causes membrane melting and expansion. We locally heated the membranes of two adjacent vesicles by laser irradiating gold nanoparticles, thus causing vesicle fusion with associated membrane and cargo mixing. The mixing time scales were consistent with diffusive mixing of the membrane dyes and the aqueous content. This method is useful for nanoscale reactions as demonstrated here by I-BAR protein-mediated membrane tubulation triggered by fusion.

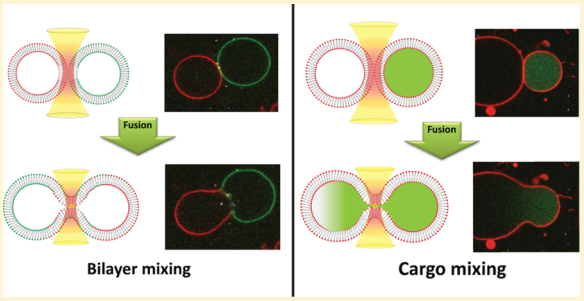


**KEYWORDS:** *vesicle, fusion, nanoparticle, optical trap, I-BAR, GUV*

The fusion of the cargos of two selected vesicles allows for controlled nanoscale reactions with femtoliter volumes, thus paving the way for single- or few-molecule reactions. This is highly useful for studying the dynamics of chemical reactions.[1] Fusion of vesicles, or fusion of vesicles with cells is the heart of liposome based targeted drug delivery, a topic of large medical interest. Fusion of one cell with another allows for the creation of hybrid cells that combines the properties of several cell types. Examples include (i) hybridoma technology,[2] which can be used to create monoclonal antibodies, (ii) combination of stem cells with differentiated cells with the potential for novel diabetes treatments through pancreatic islet transplantation,[3] or (iii) the fusion of dendritic cells to a triply negative breast cancer cell, which can be exploited for vaccine creation.[4] As fusion of vesicles and cells is of high interest, considerable effort has been put into developing efficient methods for fusion. There exists an extensive library of biological and chemical molecules that trigger fusion of cells and vesicles, for instance, cellular expressed fusogenic proteins,[5] PEG-polymers incorporated into the membranes,[6] lanthanide salts,[7] viral-based fusion peptides,[8] synaptic SNARE-mediated fusion complexes,[9] or synthetic molecular fusion complexes based on nucleotides.[10] However, fusion can also be mediated by physical means, for instance, via electrofusion[1,3,4,11] or by locally irradiating ultraviolet (UV) light on the contact area between two membranes. Cell-cell fusion can be accomplished by irradiating a cell population in medium with a high powered pulsed UV laser,[12,13] however, with limited control over the system. A more sophisticated implementation of the pulsed UV laser-mediated fusion was demonstrated for immune cells that were brought into contact via an antibody-conjugated nanoparticle.[14] The use of intense UV-laser pulses causes generation of highly reactive free radicals, which is an undesirable side-effect when dealing with live cell samples. Although such lasers are focused to a diffraction limited spot, they exhibit high divergence and still illuminate a substantial part of the cells or GUVs (giant unilamellar vesicles) both below and above the focal spot.

Here, we report on a novel and efficient method for triggering fusion of two vesicles with one critical benefit being that two vesicles can be specifically chosen among a population. The method is based on optical trapping of a metallic nanoparticle by near-infrared (NIR) light that is essentially harmless to biological material. The metallic nanoparticle will absorb part of the NIR light and the absorbed energy will be dissipated as heat in the surroundings on a length scale comparable to the diameter of the particle,[15,16] and it is this local temperature elevation that triggers membrane heating, expansion, and fusion, possibly by opening a fusion pore. Using the optical trap, two selected GUVs are manipulated and brought into close proximity.[17] After the two selected GUVs are brought into contact, the trapping of a gold nanoparticle (AuNP) in the contact zone between the GUVs causes the two vesicles to fuse by a thermally triggered mechanism. This fusion causes the membranes and the cargos of the two vesicles to mix. In contrast to fusion methods based on UV lasers, essentially no biological damage is done above nor below the focal volume. Importantly, the process can be followed real-time in a microscope. To demonstrate the general applicability of this method we also prove fusion of GUVs existing in gel and fluid phases, respectively. Finally, as a relevant biophysical application we show how protein-mediated membrane shaping

**Received:** April 9, 2015
**Revised:** May 18, 2015
**Published:** May 26, 2015





DOI: 10.1021/acs.nanolett.5b01366
*Nano Lett.* 2015, 15, 4183−4188

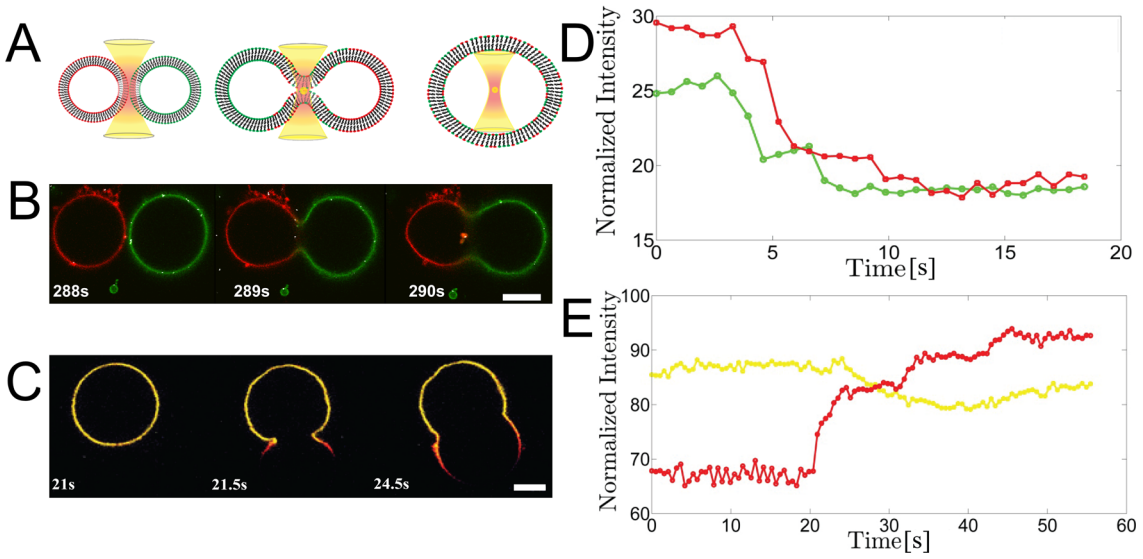


**Figure 1.** Vesicle fusion mediated by optically heated AuNPs. (A) Sketch depicting how two adjacent GUVs are fused by laser-induced heating of a AuNP trapped between the GUVs. Fusion causes a complete mixing of the lipids and the cargos. (B) Confocal images from an experiment showing the same stages as depicted in panel A. The two fluid phase DOPC/DOPS vesicles are labeled with green Fast-DiO and red TR, respectively. The scale bar is 10 $\mu$m. (C) Images showing fusion between a gel phase $DC_{15}PC$ vesicle labeled with DiI (yellow) and a fluid phase DOPC/DOPS vesicle labeled with TR (red). The dyes are only excited with a single laser line at 514 nm. The scale bar is 10 $\mu$m. (D) Normalized emitted intensities from Fast-DiO and TR from the experiment shown in panel B as a function of time. Upon fusion, the intensities decrease because the conserved number of fluorophores are diluted within a larger membrane area. (E) Normalized emitted intensities from DiI and TR from the experiment shown in panel C as a function of time; FRET occurs during the fusion process.

can be triggered by fusion and followed in real time; a neutral GUV, containing I-BAR domains, is fused to an empty GUV composed of acidic lipids and after fusion the I-BAR proteins induce membrane tubulation.

The GUVs were prepared with fluorophores and flushed into a chamber; details on the fluorophores and chamber preparation are given as Supporting Information. The chamber was mounted on a Leica SP5 confocal microscope into which an optical tweezers system based on a NIR laser was implemented.[18] The AuNPs (diameter 80 nm) were added to the chamber before the experiment started. Because of their highly inert chemical nature, the AuNPs did not interfere with GUVs within the time frame of the experiment. As previously shown, 80 nm AuNPs are efficiently trapped by focused NIR laser light and can generate high local temperatures.[15,19,20] The focused NIR laser light was used to position two vesicles of choice in close proximity to each other, as shown in Supporting Information Figure S1. The laser was typically operated with an output laser power of 1 W of which ∼200 mW reached the sample. In all experiments here shown, the vesicles contained 300 mM sucrose. Encapsulation of sucrose was necessary in order to establish a refractive index difference between the vesicle and the surrounding medium, and thereby allow for optical manipulation of individual vesicles.[17] However, we also fused vesicles containing 150− 600 mM sucrose, which did not appear to change their ability to fuse compared to the vesicles containing 300 mM sucrose. After close contact was established between the GUVs, the focus of the optical trap was positioned at the point where the membranes of the two GUVs met (as sketched in Figure 1A). One or more 80 nm AuNPs were allowed to diffuse into the focus of the laser beam; these AuNPs could either already be attached to the vesicle or be in the media and the waiting time for this to happen was typically less than 1 min. Irradiation of the AuNPs by the optical trap generated sufficient heat to transiently open the two opposing membranes resulting in rapid fusion; one such fusion event is shown in Figure 1B. Particles smaller than 80 nm were not efficient in inducing fusion, which is probably related to their smaller temperature increase upon irradiation.[15] Larger AuNPs (>150 nm) could also be used for inducing fusion, but these particles tend to become trapped off axis in local intensity maxima originating from spherical aberration.[21]

In the experiment shown in Figure 1B, all vesicles were made from the same DOPC/DOPS mixture, all were in fluid phase, some of the vesicles were labeled green (with Fast-DiO), and others were labeled red with Texas Red DHPE (TR). All vesicles contained 300 mM sucrose so that they could be easily optically trapped. One green and one red GUV were selected and brought into close proximity, whereafter a AuNP diffused into the trap, heated, and caused fusion of the membranes. Upon fusion, the membranes of the vesicles mix. This can be seen from Figure 1D that upon fusion shows a clear decrease in emitted intensity per area of both the green and red membrane incorporated dyes because of the increased membrane area. For fluid membranes, the lipid mixing occurs within ∼10 s for typical vesicle sizes of 20 $\mu$m.

Fusion of GUVs by this methodology is not limited to fluid vesicles but can also be accomplished between a fluid phase DOPC/DOPS vesicle and a gel phase $DC_{15}PC$ vesicle, as shown in Figure 1C (fluid phase is labeled red with TR and gel phase yellow with DiI). As the chosen pair of fluorophores has a spectral overlap, a fluorescence resonance energy transfer (FRET) occurs during fusion because the donor molecules (DiI) and the acceptor molecules (TR) slowly migrate and mix. Such a FRET transfer is shown in Figure 1E. The time scale of mixing of lipids between gel and fluid phase GUVs was measured to be significantly slower (∼50 s in Figure 1E) than the lipid−lipid mixing between fluid phase membranes (∼10 s in Figure 1D), which is consistent with the much slower diffusion of lipids in gel phase membranes. Also, we found that



DOI: 10.1021/acs.nanolett.5b01366
*Nano Lett.* 2015, 15, 4183−4188

two gel phase vesicles could be fused (shown in Supporting Information Figure S2).

Fusion was easily performed between vesicles ranging in size from ~10−200 $\mu$m, where the lower limit is set by the scattering forces from the optical trap which hinder simultaneous positioning of small GUVs and AuNPs within the same focal plane. The upper limit of this interval (200 $\mu$m) was simply set by the vesicle production method (electroformation or gel-assisted hydration), which did not produce vesicles larger than 200 $\mu$m. It is likely that the proposed fusion method will also work well for larger vesicles. To minimize the adhesion of GUVs to surfaces and thereby facilitate optical manipulation of the GUVs we passivated the sample with $\alpha$-casein. Passivation of the glass with $\alpha$-casein also minimizes an adhesion induced increase in membrane tension that may affect the probability of fusion.[22]

To quantify the time scales of membrane mixing in fluid phase DOPC/DOPS vesicles during fusion we labeled one batch of vesicles with TR and a second batch with a Fast-DiO cyanine dye. These two dyes do not have significant spectral overlap hence the FRET is minimal. By methods, as shown in Figure 1D, we measured typical equilibration time scales on the order of 10 s; however, the exact time scale for complete mixing depended on the sizes of the fusing vesicles. Figure 2 shows the relation between the size of the vesicle fused to the vesicle containing the fluorophore of interest and the time scale of mixing Fast-DiO and TR, respectively. There is a linear relation between the added area, $r^2$, and the mixing time scale, $t$. Such a linear relation is predicted by the normal diffusion equation, $\langle r^2\rangle^{1/2} = (4Dt)^{1/2}$, where $D$ is the diffusion constant of the fluorophore. However, this diffusion model describes diffusion in unlimited areas with reservoirs of fluorophores and therefore it does not adequately describe our system which consists of two fusing GUVs with finite areas and finite numbers of fluorophores. However, from Figure 2A it is clear that DiO diffuses significantly faster than TR. Simple fits to the slopes in Figure 2A provide upper limit estimates of $D_{TR}$ and $D_{DiO}$. These estimates are a factor of 10 larger than literature values measured by FRAP (fluorescence recovery after photobleaching) in GUVs and in tethered bilayers,[23−25] which for TR range from $D_{TR}$ = 2 $\mu$m$^2$/s to $D_{TR}$ =6.5 $\mu$m$^2$/s and for DiO was found to be $D_{DiO}$ ~ 15 $\mu$m$^2$/s[26] (according to the webpage on DiO from "Life Technologies" the value given in ref 26 should be multiplied by a factor of 2).

Also, we compared our data with a more relevant model that was previously used to study diffusion of lipid fluororophores in GUVs.[27] This model describes mixing of lipophilic fluorophores in a situation where all fluorophores are initially confined in one hemisphere of a spherical shell and at time zero are free to diffuse over the entire shell. This situation is described by the following diffusion equation (cast in spherical coordinates)[27]

$$\partial_t c = D\frac{1}{r^2\sin(\theta)}\partial_\theta \sin(\theta)\partial_\theta c \tag{1}$$

where it is assumed that $c$, the concentration, does not depend on radius, $r$, nor on the angle, $\phi$, but only on $\theta$ (see inset of Figure 2B for definitions of the angles $\phi$ and $\theta$). A solution of eq 1 is given in ref 27 and the average concentrations in the two hemispheres are given by

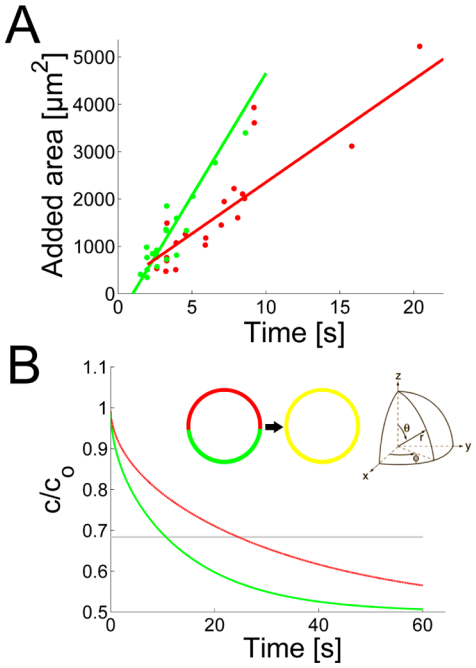


**Figure 2.** Correlation between added membrane area and mixing time scales during fusion. (A) Experimental data showing how the area added to a liquid phase vesicle containing TR (red symbols) or Fast-DiO (green symbols) during fusion correlates with the mixing time scale. (B) Equilibration of fluorophore concentrations calculated via a theoretical model of diffusion from one hemisphere into the other hemisphere of radius 21.1 $\mu$m.[27] This size is chosen because the area of the hemisphere then corresponds to the median size of the added membrane area in the experiments depicted in panel A. The red line in panel B is calculated using $D_{TR}$ = 6.5 $\mu$m$^2$/s and the green line using $D_{DiO}$ = 15 $\mu$m$^2$/s. The horizontal gray line shows the level where the concentration has equilibrated to a fraction of $1/e$ of the initial concentration; the crossing of this line with the curves can be compared to the mixing time scales from the experiments plotted in panel A. The left inset illustrates the model and the right inset explains the spherical coordinates used.

$$c_{\pm}(t) = \frac{\alpha+\beta}{2} \pm \frac{\alpha-\beta}{2}\sum_{k=0}^{\infty} P_k e^{-(2k+1)(2k+2)(D/r^2)t} \tag{2}$$

where $\alpha$ and $\beta$ are the initial fluorophore concentrations in the two halves and $D$ is the diffusion constant. $P_k$ is given by

$$P_k = (4k+3)\left\{\frac{(2k)!}{2^{2k+1}k!(k+1)!}\right\}^2 \tag{3}$$

By assuming $\alpha$ = 0 and $\beta$ = 1 we get the equilibration of fluorophore concentration, $c(t)$, as plotted in Figure 2B for a shell with radius 21.1 $\mu$m (area of 5572 $\mu$m$^2$). Because we model two fusing GUVs this size was chosen to be a shell having twice the median area of the GUVs used in the experiments (2786 $\mu$m$^2$) in Figure 2A. Using the literature values given above, $D_{DiO}$ = 15 $\mu$m$^2$/s and $D_{TR}$ = 6.5 $\mu$m$^2$/s, the theoretical mixing time scale (where the horizontal line intersects the curves in Figure 2B) are found to be 10.6 and 24.5 s for DiO and TR, respectively. These numbers are relatively close to the experimentally measured ones for a similarly sized added vesicle (see Figure 2A) and thus confirm lipid mixing of the two fluid phase GUVs.

Hot nanoparticle induced fusion of two GUVs causes a complete fusion, also of their lumens. We here demonstrate



DOI: 10.1021/acs.nanolett.5b01366
Nano Lett. 2015, 15, 4183−4188

how this can be used to study mixing of the two lumens and chemical reactions induced by the fusion. We fused a GUV containing a mixture of sucrose and calcein with a GUV that only contained a sucrose solution; the experiment is sketched in Figure 3A and images from the experiment are shown in Figure

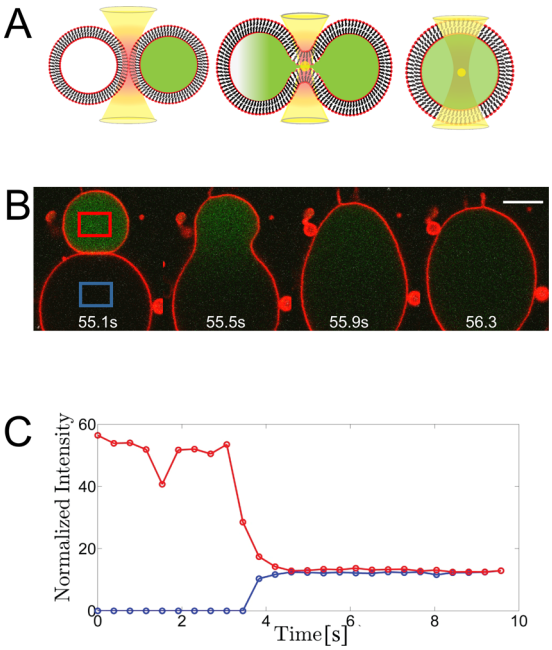


**Figure 3.** Lumen mixing during vesicle fusion. (A) Sketch of the fusion process. (B) Confocal images of the fusion process of two fluid phase GUVs with their membranes marked by TR, one GUV contains only a sucrose solution, the other sucrose mixed with calcein (green). The scale bar is 10 $\mu$m. (C) Intensity emitted by calcein in the two boxed regions in panel B, red trace (from red box) is from a region that starts out being inside the calcein containing vesicle, blue trace (from blue box) is from a region that starts out being in the empty vesicle. Approximately ∼0.3−0.5 s after fusion the calcein intensity distribution is uniform within the fused GUV.

3B. By monitoring the emission of calcein in two regions, corresponding to the lumens of the two original GUVs, we quantified how calcein diffused from the calcein containing GUV (red line in Figure 3C) and into the lumen of the empty GUV (blue line in Figure 3C) upon fusion. After less than 0.5 s, calcein was uniformly distributed in the fused lumen. This time scale is expected for three-dimensional diffusion of calcein across a distance corresponding to the size of the GUV (∼20 $\mu$m) assuming a diffusion constant of calcein in water of roughly 200 $\mu m^2/s$.[28] As expected, we also found that the intensity of calcein emission in the fused lumen was proportional to the ratio between the volumes of the calcein containing vesicle and the volume of the fused vesicle, this is shown in Supporting Information Figure S3. This type of experiment demonstrates that chemical reactions between reactants encapsulated within picoliter volumes can be studied, for example, via fluorescence microscopy that can reach a time resolution of acquisition of ∼5 ms.

The vesicle fusion assay here presented has great potential for triggering and monitoring protein interactions in GUVs. By first encapsulating proteins within one GUV with an inert composition and subsequently fusing to another GUV containing a lumen or membrane composition that activates the function of the protein, it is possible to activate the protein in a controlled manner and study the activity of the protein in real time. We here demonstrate this using the curvature-inducing domain of the peripheral membrane proteins from the I-BAR family which only binds to acidic membranes. I-BAR belongs to a large family of BAR-domain (Bin, Amphiphysin, Rvs) proteins involved in membrane curvature sensing and induction. The subset of this family called I-BAR proteins all share an N-terminal domain (an IRSp53-MIM domain), which is known to induce negative membrane curvature (e.g., protrusions such as filopodia) through a combined hydrophobic (helix) domain insertion and electrostatic attraction to negatively charged acidic phospholipids.[29] The basic patch in both ABBA and MIM carries basic lysine and arginine amino acid residues that facilitate efficient binding to negative membranes.

To study the membrane binding of the I-BAR we encapsulated I-BAR-proteins within GUVs composed of zwitterionic lipids for which no protein binding occurs, details of the encapsulation procedure are given in the Supporting Information. In Figure 4, all three panels show the fusion of an I-BAR-containing vesicle to a GUV composed of a mixture of DOPC and negatively charged DOPS; before fusion tubulation is absent but after fusion the tubulation activity is clearly present. We also observed tube formation with GUVs containing different negative lipid species such as phosphoinositide lipids with several negative charges for each headgroup, see Figure 4B. Additional examples of I-BAR mediated tubulation following fusion are shown as Supporting Information Figures S4 and S5.

Biophysical studies of I-BAR protein activity have mainly been done through fluorescent imaging while adding the protein globally to a solution of vesicles and these studies have reported an inward directed tubulation.[30,31] Also, I-BAR has been shown by cryo-electron microscopy to induce tubules of specific radii that were found to be 55−60 nm in diameter.[30] Until now, however, it has not been possible to measure the kinetics of tube formation in real time and, more importantly, I-BAR was always added to the outside of the spherical membranes resulting in inward directed tubes although its natural presence in cells is inside filopodia that protrude outward. The assay presented here thus allows studying I-BAR in real time and with the protein encapsulated inside a spherical membrane.

Fusion of GUVs existing in different physical states and, containing various lipophilic and aqueous fluorophores, can be readily performed allowing lipid and content mixing to be monitored in real-time. The mechanism behind the membrane fusion assay is most likely a thermally induced opening of the membrane followed by fusion of the apposing membranes. The membrane area per headgroup expands ca. 0.5% per degree when lipids are in a fluid phase.[32] As the 80 nm gold nanoparticle is trapped with a laser power of ∼200 mW, the temperature of the gold nanoparticle easily reaches ∼75 °C,[15] however, if the particle is displaced from the center of the trap its surface temperature will be lower[20] and if several particles aggregate their temperature will be higher. The high local temperature increase is sufficient to increase the distance between adjacent neighboring lipids, and the consequent exposure of the hydrophobic bilayer core could therefore well be the mechanism responsible for fusion. The fusion between gel phase GUVs in Figure 1C (fluid−gel) and Supporting Information Figure S2 (gel−gel) shows that it is indeed possible to induce fusion of rigid GUVs that locally melt to


DOI: 10.1021/acs.nanolett.5b01366
Nano Lett. 2015, 15, 4183−4188

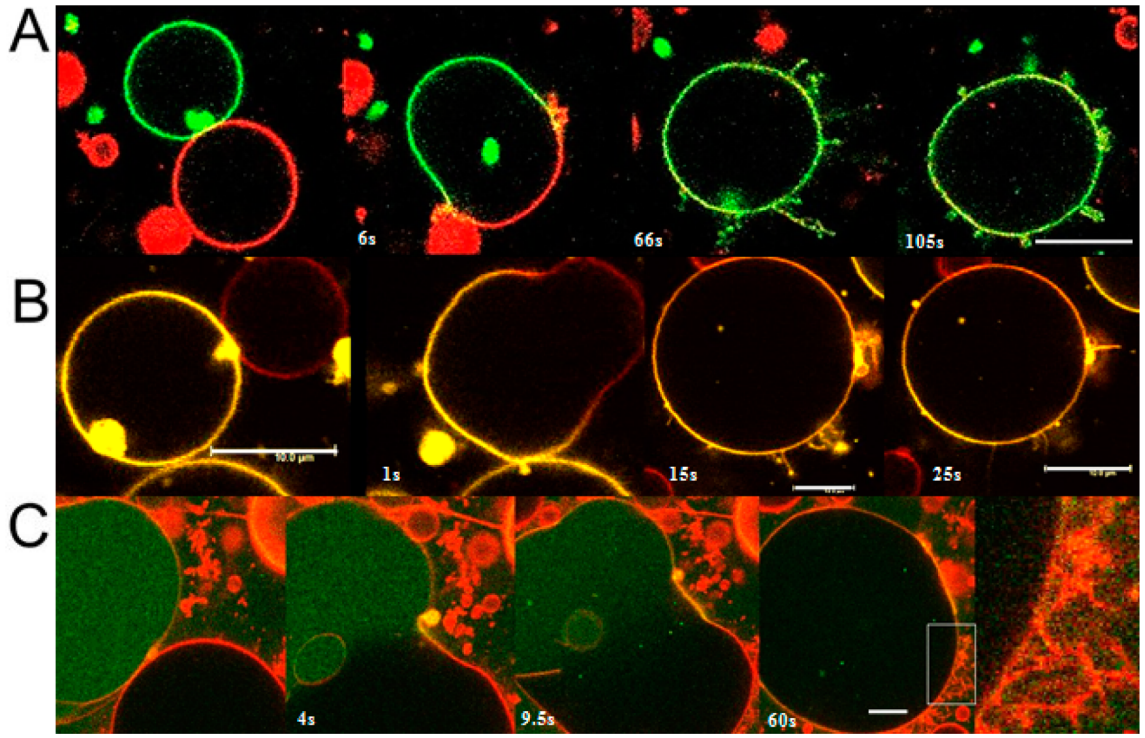


**Figure 4.** Fusion of acidic vesicles with neutrally charged GUVs containing I-BAR protein. Upon fusion membrane tubulation is induced. (A) A Fast-DiO-labeled neutral DOPC vesicle (green) containing ABBA I-BAR-protein is fused to a TR-labeled acidic vesicle (red) with 40% DOPS lipids. After fusion several distinct protruding tubes appear. (B) A DiD-labeled DOPC vesicle (red) containing MIM I-BAR-protein is fused with a TR-labeled (yellow) DOPC vesicle containing 10 mol % PI(4,5)P2 lipids. Protruding tubules are observed immediately after fusion. (C) A DiD-labeled DOPC vesicle (red) containing YFP-tagged ABBA protein (green lumen) is fused with a DiD-labeled vesicle with 30% DOPS lipids (this vesicle is also red but has a black lumen). In this experiment, the concentration of ABBA I-BAR-protein used for encapsulation is ~10× higher than in panel A and a correspondingly larger population of tubules are formed after fusion. The YFP tagged ABBA protein dilutes and bleaches within seconds.

initiate the fusion process. Gel phase membranes expand even more when heated in particular when the temperature is increased above the phase transition temperature at which the bilayer expands around 20−25%.[33]

The ability to mix the cargoes within two selected GUVs has great implications for conducting and monitoring chemistry at microscale. Because hydrophilic molecules can be easily encapsulated within attoliter liposomes, we envision that our strategy can be further developed to achieve fusion of much smaller volumes and pave the way to attoliter nanoscale chemistry. This could for instance be done by conjugating AuNPs to the lipid headgroups and wait for small liposomes to colocalize within the optical trap and fuse. The method demonstrated here is extremely flexible and can in principle be applied to all membrane structures suspended in a fluid chamber. Exciting future applications also include fusion of GUVs containing a certain cargo to be delivered within living cells. For many applications it is desirable to be able to decide exactly which cell, potentially exhibiting a certain protein expression, should be fused with which vesicle. In conclusion, the results here presented pave the way for future use of plasmon mediated vesicle fusion to fuse with synthetic vesicles or with live cells, thus allowing for on demand delivery of chemical or genetic material to cells or the formation of hybrid cells.

## ■ ASSOCIATED CONTENT

### Supporting Information

The Supporting Information is available free of charge on the ACS Publications website at DOI: 10.1021/acs.nanolett.5b01366.

## ■ AUTHOR INFORMATION

### Corresponding Authors

*E-mail: oddershede@nbi.dk.
*E-mail: bendix@nbi.dk.

### Notes

The authors declare no competing financial interest.

## ■ ACKNOWLEDGMENTS

We thank P. Lappalainen, University of Helsinki, for kindly providing the plasmids for the I-BAR proteins. We acknowledge financial support from the Villum Kann Rasmussen Foundation, the Lundbeck Foundation, StemPhys and C-mol (DNRF Centers of Excellence), and from the Danish Research Councils.

## ■ REFERENCES

(1) Yang, P.; Lipowsky, R.; Dimova, R. *Small* **2009**, *5*, 2033−2037.
(2) Milstein, C. *Bioessays* **1999**, *21*, 966−973.
(3) Yanai, G.; Hayashi, T.; Zhi, Q.; Yang, K.-C.; Shirouzu, Y.; Shimabukuro, T.; Hiura, A.; Inoue, K.; Sumi, S. *PLoS One* **2013**, *8*, e64499.
(4) Zhang, P.; Yi, S.; Li, X.; Liu, R.; Jiang, H.; Huang, Z.; Liu, Y.; Wu, J.; Huang, Y. *PLoS One* **2014**, *9*, e102197.



DOI: 10.1021/acs.nanolett.5b01366
*Nano Lett.* 2015, 15, 4183−4188

(5) Kouris, N. A.; Schaefer, J. A.; Hatta, M.; Freeman, B. T.; Kamp, T. J.; Kawaoka, Y.; Ogle, B. M. *Stem Cells Int.* **2012**, *2012*, 13.
(6) Tarafdar, P. K.; Chakraborty, H.; Dennison, S. M.; Lentz, B. R. *Biophys. J.* **2012**, *103*, 1880−1889.
(7) Tanaka, T.; Yamazaki, M. *Langmuir* **2004**, *20*, 5160−5164.
(8) Harrison, S. C. *Nat. Struct. Mol. Biol.* **2008**, *15*, 690−698.
(9) Martens, S.; McMahon, H. T. *Nat. Rev. Mol. Cell Biol.* **2008**, *9*, 543−556.
(10) van Lengerich, B.; Rawle, R. J.; Bendix, P. M.; Boxer, S. G. *Biophys. J.* **2013**, *105*, 409−419.
(11) Dimova, R.; Riske, K. A.; Aranda, S.; Bezlyepkina, N.; Knorr, R. L.; Lipowsky, R. *Soft Matter* **2007**, *3*, 817−827.
(12) Wiegand, R.; Weber, G.; Zimmermann, K.; Monajembashi, S.; Wolfrum, J.; Greulich, K. O. *J. Cell Sci.* **1987**, *88*, 145−149.
(13) Steubing, R. W.; Cheng, S.; Wright, W. H.; Numajiri, Y.; Berns, M. W. *Cytometry* **1991**, *12*, 505−510.
(14) Yeheskely-Hayon, D.; Minai, L.; Golan, L.; Dann, E. J.; Yelin, D. *Small* **2013**, *9*, 3771−3777.
(15) Bendix, P. M.; Nader, S.; Reihani, S.; Oddershede, L. B. *ACS Nano* **2010**, *4*, 2256−2262.
(16) Bendix, P. M.; Jauffred, L.; Norregaard, K.; Oddershede, L. B. *IEEE J. Sel. Top. Quantum Electron.* **2014**, *20*, 4800112.
(17) Bendix, P. M.; Oddershede, L. B. *Nano Lett.* **2011**, *11*, 5431−5437.
(18) Richardson, A. C.; Reihani, N.; Oddershede, L. B. *SPIE Proc.* **2006**, *6326*, 28−38.
(19) Hansen, P. M.; Bhatia, V. K.; Harrit, N.; Oddershede, L. *Nano Lett.* **2005**, *5*, 1937−1942.
(20) Kyrsting, A.; Bendix, P. M.; Stamou, D. G.; Oddershede, L. B. *Nano Lett.* **2011**, *11*, 888−892.
(21) Kyrsting, A.; Bendix, P. M.; Oddershede, L. B. *Nano Lett.* **2013**, *13*, 31−35.
(22) Shillcock, J. C.; Lipowsky, R. *Nat. Mater.* **2005**, *4*, 225−228.
(23) Diaz, A. J.; Albertorio, F.; Daniel, S.; Cremer, P. S. *Langmuir* **2008**, *24*, 6820−6826.
(24) Chung, M.; Lowe, R. D.; Chan, Y. H. M.; Ganesan, P. V.; Boxer, S. G. *J. Struct Biol.* **2009**, *168*, 190−199.
(25) Ciobanasu, C.; Siebrasse, J. P.; Kubitscheck, U. *Biophys. J.* **2010**, *99*, 153−162.
(26) Doeven, M. K.; Folgering, J. H. A.; Krasnikov, V.; Geertsma, E. R.; van den Bogaart, G.; Poolman, B. *Biophys. J.* **2005**, *88*, 1134−1142.
(27) Peters, R.; Peters, J.; Tews, K. H.; Bahr, W. *Biochim. Biophys. Acta* **1974**, *367*, 282−294.
(28) Wang, T.; Smith, E. A.; Chapman, E. R.; Weisshaar, J. C. *Biophys. J.* **2009**, *96*, 4122−4131.
(29) Lee, S. H.; Kerff, F.; Chereau, D.; Ferron, F.; Klug, A.; Dominguez, R. *Structure* **2007**, *15*, 145−155.
(30) Saarikangas, J.; Zhao, H.; Pykalainen, A.; Laurinmaki, P.; Mattila, P. K.; Kinnunen, P. K.; Butcher, S. J.; Lappalainen, P. *Curr. Biol.* **2009**, *19*, 95−107.
(31) Linkner, J.; Witte, G.; Zhao, H. X.; Junemann, A.; Nordholz, B.; Runge-Wollmann, P.; Lappalainen, P.; Faix, J. *J. Cell Sci.* **2014**, *127*, 1279−1292.
(32) Pan, J.; Heberle, F. A.; Tristram-Nagle, S.; Szymanski, M.; Koepfinger, M.; Katsaras, J.; Kucerka, N. *Biochim. Biophys. Acta* **2012**, *1818*, 2135−2148.
(33) Schuy, S.; Janshoff, A. *ChemPhysChem* **2006**, *7*, 1207−1210.



DOI: 10.1021/acs.nanolett.5b01366
*Nano Lett.* 2015, 15, 4183−4188